Structure
with Folding with Design

Three new crystal structures of point mutation variants of mono TIM: conformational flexibility of loop -1, loop -4 and loop -8

[Research Article]

Torben V Borchert, KV Radha Kishan, Johan Ph Zeelen, Wolfgang Schliebs, Narmada Thanki, Ruben Abagyan, Rainer Jaenicke, Rik K Wierenga

Structure 1995, **3**:669-679.

Text only, **+ full figures**

Publications by
Rik K Wierenga | Rainer Jaenicke | Ruben Abagyan | Narmada Thanki | Wolfgang Schliebs | Johan Ph Zeelen | KV Radha Kishan | Torben V Borchert

Jump to this record in Evaluated MEDLINE
Related records from Evaluated MEDLINE
Related fulltext articles on BioMedNet

Outline

Abstract

Backgound

Wild-type triosephosphate isomerase (TIM) is a very stable dimeric enzyme. This dimer can be converted into a stable monomeric protein (monoTIM) by replacing the 15-residue interface loop (loop-3) by a shorter, 8-residue, loop. The crystal structure of monoTIM shows that two active-site loops (loop-1 and loop-4), which are at the dimer interface in wild-type TIM, have acquired rather different structural properties. Nevertheless, mono TIM has residual catalytic activity.

Results

Three new structures of variants of monoTIM are presented, a double-point mutant crystallized in the presence and absence of bound inhibitor, and a single-point mutant in the presence of a different inhibitor. These new structures show large structural variability for the active-site loops, loop-1, loop-4 and loop-8. In the structures with inhibitor bound, the catalytic lysine (Lys13 in loop-1) and the catalytic histidine (His95 in loop-4) adopt conformations similar to those observed in wild-type TIM, but very different from the mono TIM structure.

Conclusion

The residual catalytic activity of monoTIM can now be rationalized. In the presence of substrate analogues the active-site loops, loop-1, loop-4 and loop-8, as well as the catalytic residues, adopt conformations similar to those seen in the wild-type protein. These loops lack conformational flexibility in wild-type TIM. The data suggest that the rigidity of these loops in wild-type TIM, resulting from subunit–subunit contacts at the dimer interface, is important for optimal catalysis.

Keywords

- assembly
- flexibility
- loops
- subunit
- triosephosphate isomerase (TIM)

Introduction

Triosephosphate isomerase (TIM) is a dimeric glycolytic enzyme consisting of two identical subunits. It catalyzes the interconversion of dihydroxyacetone phosphate and D-glyceraldehyde-3-phosphate [1] (Fig. 1a). Each subunit consists of eight ($\beta\alpha$) units (Fig. 2), forming a buried barrel of eight parallel β-strands (strands B1–8), covered on the outside by eight α-helices (helices H1–8). The loops immediately following the β-strands (referred to as loops L1–8) have important functional properties. These loops are near the active site [2] [3] and loops L1–4 (collectively referred to as the interface loops) are also involved in interactions across the dimer interface [3]. Loops L3 and L6 protrude from the monomeric subunit; L3 docks into a groove between L1 and L4 of the other subunit, near the active site of this subunit. In wild-type TIM (wtTIM) only one interaction occurs between L1 and L4 of the same subunit — a conserved salt bridge between Lys13 (L1) and Glu97 (L4). Loop L6 extends into the surrounding solution in the absence of ligand — the so-called 'open' form — but closes off the active site (the so-called 'closed' form), once a ligand has been bound in the active site [4]. Loops L1–8 are at the 'business' end of the molecule; we will refer to these loops as the 'front' loops. Important catalytic residues are Lys13 in L1, His95 in L4 and Glu167 in L6 (Fig. 2). The 'back' loops preceding the β-strands are located on the other side of the molecule and may be important for the stability of the TIM barrel [5].

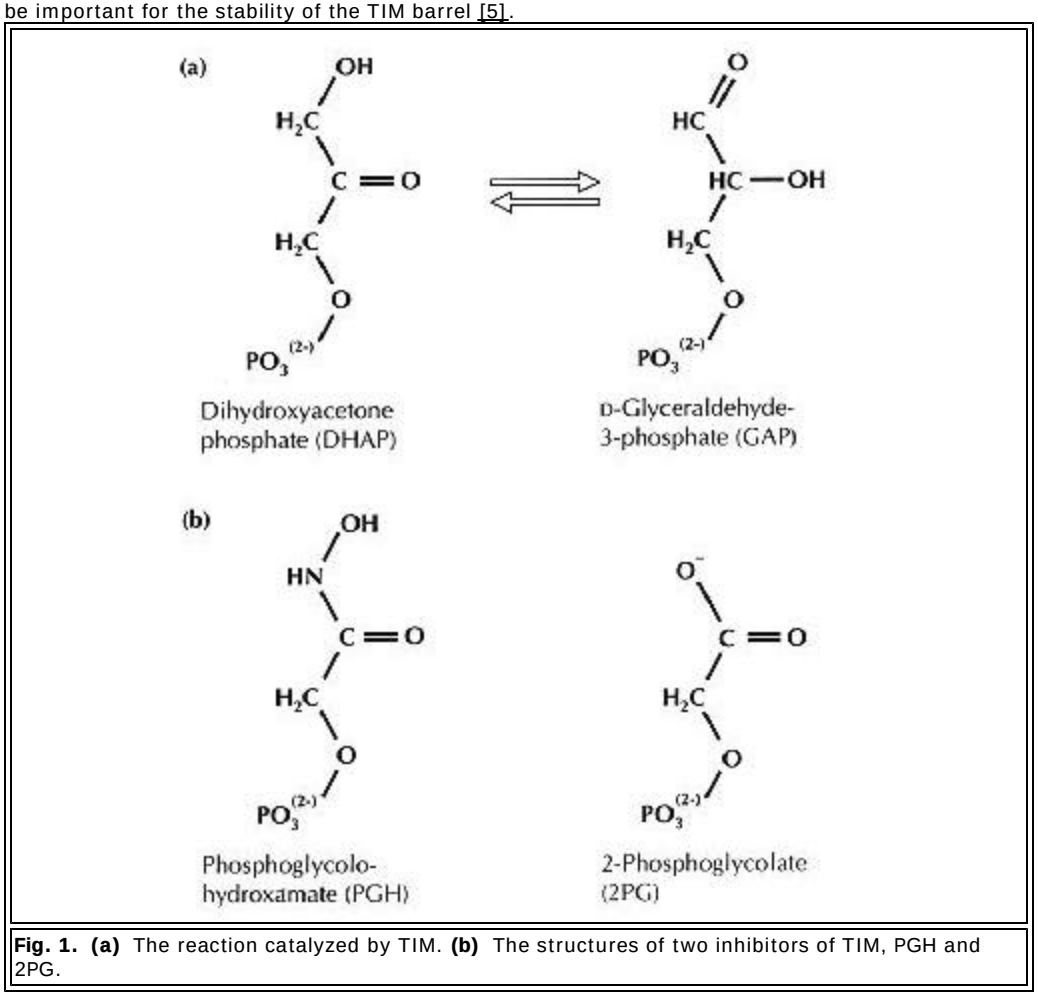

Fig. 1. (a) The reaction catalyzed by TIM. **(b)** The structures of two inhibitors of TIM, PGH and 2PG.

Return to text reference [1] [2] [3]

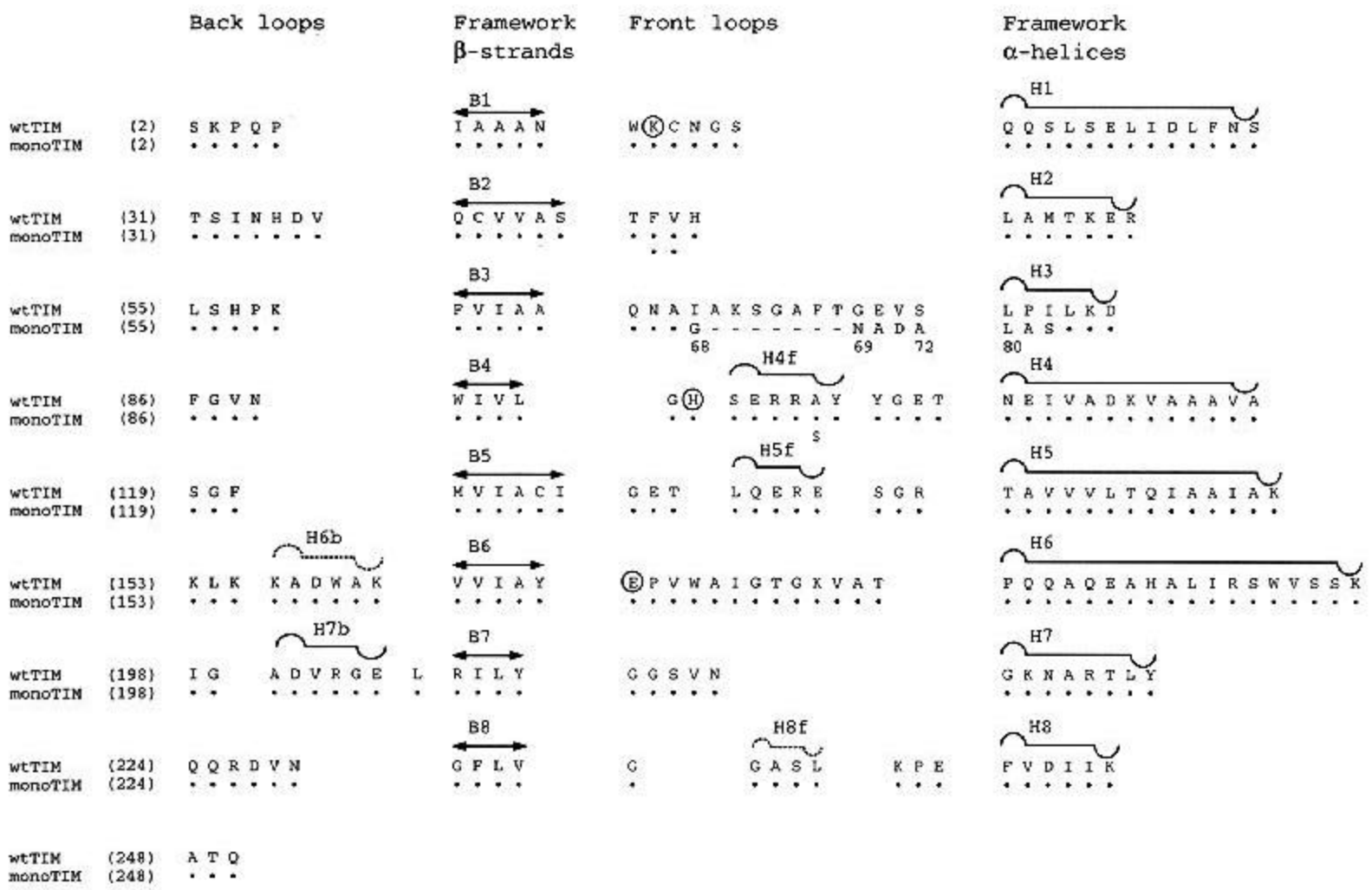

Fig. 2. The sequence and numbering of wild-type (wt) TIM and mono TIM. The sequence of mono TIM is the same as for trypanosomal TIM (as indicated by dots), except near front loop L3, where seven residues have been deleted (-) and a number of sequence changes introduced. The residue-numbering scheme for mono TIM is indicated below the sequence. Mono TIM-SS differs from mono TIM in front loop L2 (at the positions indicated by the two asterisks); the sequence changes are Phe45⟶Ser and Val46⟶Ser. Mono TIM-W differs from mono TIM in front loop L4 (at the position indicated by); the sequence change is Ala100⟶Trp. The circled residues are the catalytic residues Lys13, His95 and Glu167. The β-strands and α-helices are indicated by solid lines. The dotted lines indicate 3_{10}-helices. H4f, H5f, H8f, H6b and H7b are helical fragments in the respective loops.

Return to text reference [1] [2] [3] [4] [5] [6]

Monomeric TIM (MonoTIM) has been derived from trypanosomal TIM by shortening the major dimer interface loop, L3, by seven residues. It has been shown that monoTIM is a stable monomeric protein with residual catalytic activity [6]. Its turnover number (k_{cat}) is about 1000 times lower when compared with that measured for wtTIM, and the Michaelis constant (K_M) is 10 times higher. As TIM has a very high turnover number (k_{cat} is 3.7×10^5 min^{-1}) [7] this implies that mono TIM retains

considerable catalytic activity.

The crystal structure of mono TIM has been determined with a sulphate ion bound in the active site [8]. Important differences between the structures of monoTIM and wtTIM include the increased flexibility of the residues Lys13-Cys14-Asn15 in L1 of monoTIM (there is no electron density for these residues) and the very different structure of L4 (residues 94–104). In monoTIM, the side chain of the catalytic histidine (His95 in L4) points away from the active site instead of towards it as in wtTIM (the distance between the NE2 side-chain atoms in the two different conformations is 12 Å).

The considerable catalytic activity of monoTIM relative to wtTIM is not readily understood on the basis of its crystal structure because two catalytic residues, Lys13 in L1, and His95 in L4, have acquired very different structural properties. In wtTIM, loops L1 and L4 are stabilized by the dimer-interface interactions, which are quite extensive [3]. It has been speculated that, in solution, these loops in monoTIM will be mobile and that the solved crystal structure of monoTIM shows only one of the low-energy conformations of these loops [8]. To address these issues, we have attempted to crystallize a number of variants of monoTIM in the absence and presence of active-site ligands. Structural properties of two variants of monoTIM are discussed.

In the first variant, monoTIM-SS, two hydrophobic surface residues of monoTIM, Phe45 and Val46, have been replaced by serines. The choice of these mutations was guided by a previous study [9] of crystal contacts in four different crystal forms of wtTIM. In that analysis it was shown that serines preferentially occur in crystal contact areas. This suggested that changing hydrophobic surface residues into serines might result in new crystal forms. The second variant, monoTIM-W, is a single-site mutant (Ala100→Trp) of monoTIM. Ala100 is located in the helical fragment of loop L4 in monoTIM (Fig. 2). In monoTIM, this residue is rather buried and a tryptophan side chain is not allowed because it would come into too close contact with other atoms. However, in wtTIM (in which this helical fragment has shifted into another position) the Ala100→Trp mutation does not cause any clashes. It was anticipated that the Ala100→Trp in mutation in monoTIM would favour the wild-type conformation of L4. In wtTIM, the Ala100→Trp mutation has no effect on catalytic activity or structure (data not shown).

Measurements of the catalytic constants of monoTIM, monoTIM-SS and monoTIM-W show very similar values for k_{cat} and K_M. The approximate values are 3.5×10^2 min^{-1} and 4.4 mM, respectively (W Schliebs and RK Wierenga, unpublished data). Apparently, these mutations do not affect the catalytic properties of the active-site residues.

In this paper we report the crystal structures of monoTIM-SS in the absence of bound ligand (hereafter referred to as monoTIM-SS), monoTIM-SS in complex with phosphoglycolohydroxamate (PGH) and monoTIM-W in complex with 2-phosphoglycolate (2PG). PGH and 2PG (Fig. 1b) are the best known inhibitors of TIM, with inhibitory constant (K_i) values of ~10 μM. The three crystal forms, diffracting to approximately 2.4 Å resolution, are different from each other and from the monoTIM crystal forms (Table 1). Structural comparisons of monoTIM, monoTIM-SS, monoTIM-SS(PGH) and monoTIM-W(2PG) reveal considerable structural flexibility for loops L1, L4 and L8, and allow us to gain a better understanding of the residual catalytic activity of monoTIM and its variants.

Table 1. Crystallization conditions and crystal properties of the four monomeric TIMs.

	monoTIM	**monoTIM -SS**	**monoTIM -SS (PGH)**	**monoTIM -W (2PG)**
Buffer	100 mM MES	100 mM Tris-HCl	100 mM MES	100 mM MES
pH	6.2	8.5	6.5	6.5
Temperature (°C)	12	20	20	20

Additives	5 mM DTT, 1mM EDTA	1 mM DTT, 1mM EDTA	1 mM DTT, 1mM EDTA	1 mM DTT, 1mM EDTA
	1 mM NaN_3	1 mM NaN_3	1 mM NaN_3	1 mM NaN_3
		5% MPD		
	180 mM Li_2SO_4		15 mM PGH	3 mM 2PG
Precipitant	26% PEG6000	10% PEG8000	33% PEG6000	22% PEG6000
Space group	C2	P1	$P2_1$	C2
Max. resolution (Å)	2.4	2.4	2.4	2.4
Cell dimensions (Å)	83.8, 42.8, 68.8	46.6, 46.6, 66.7	47.1, 39.3, 68.3	78.8, 46.8, 70.4
(°)	90, 108.2, 90	94.5, 69.8, 75.8	90, 117.5, 90	90, 114, 90

Abbreviations: DTT, dithiothreitol (reduced); MES, 2-[*N*-morpholino]ethanesulphonic acid; MPD, 2-methyl-2,4-pentanediol; PEG, polyethylene glycol; 2PG, 2-phosphoglycolate; PGH, phosphoglycolohydroxamate.

Return to table reference [1] [2] [3]

Results

The crystal structures of the three monomeric TIMs have been refined to models with good geometry and low R-factors (Table 2). For the three structures the (Φ,Ψ) values are in the allowed regions of the Ramachandran plot, except for a few residues in the high B-factor regions of loops L1 and L3. Their most important structural features are described below and compared with the previously refined structures of monoTIM (in complex with sulphate) and wtTIM, with and without an active-site ligand.

Table 2. Crystallographic data.

	monoTIM -SS	**monoTIM -SS(PGH)**	**monoTIM -W(2PG)**
Space group	P1	$P2_1$	C2
No. of molecules per asymmetric unit	2	1	1
V_m ($Å^3\ D^{-1}$)	2.5	2.2	2.6
Observed reflections	22787	20243	11293
Unique reflections	13847	8529	7034
R_{merge}* (%)	4.4	5.3	6.5
Overall completeness at 2.4 Å (%)	71	86	75
Last shell			
completeness (%)	20	74	25
(resolution in Å)	(2.6–2.4)	(2.5–2.4)	(2.6–2.4)
Refinement data:			
No. of protein atoms	3642	1771	1794
No. of solvent atoms	56	40	12

No. of ligand atoms		10	9
R_{factor} † (%)	19.8	17.8	17.8
Rms bond length deviations (Å)	0.010	0.010	0.020
Rms bond angle deviations (°)	0.8	1.7	2.3

*$R_{merge} = [\sum_h \sum_i |\langle I \rangle_h - I_{h,i}| / \langle I \rangle_h]$.

†$R_{factor} = [\sum ||F_{OBS}| - |F_{CALC}|| / \sum |F_{OBS}|]$.

Return to table reference [1] [2] [3] [4] [5]

Structure of monoTIM -SS (in the absence of ligand)

In this crystal form there are two molecules per asymmetric unit. A continuous polypeptide chain could be built for both molecules, and both have the same conformation. Molecule 1 has been used for the comparison studies. The structures of the front loops are remarkably different from those of monoTIM (see Fig. 3, Fig. 4a; kinemage) and only insignificant differences occur elsewhere in the molecule. In particular, loops L6, L4 and L8 exhibit the greatest differences in Cα positions of 7 Å, 5 Å and 5 Å respectively, and loop L1, which was mobile in monoTIM, can be built in monoTIM-SS.

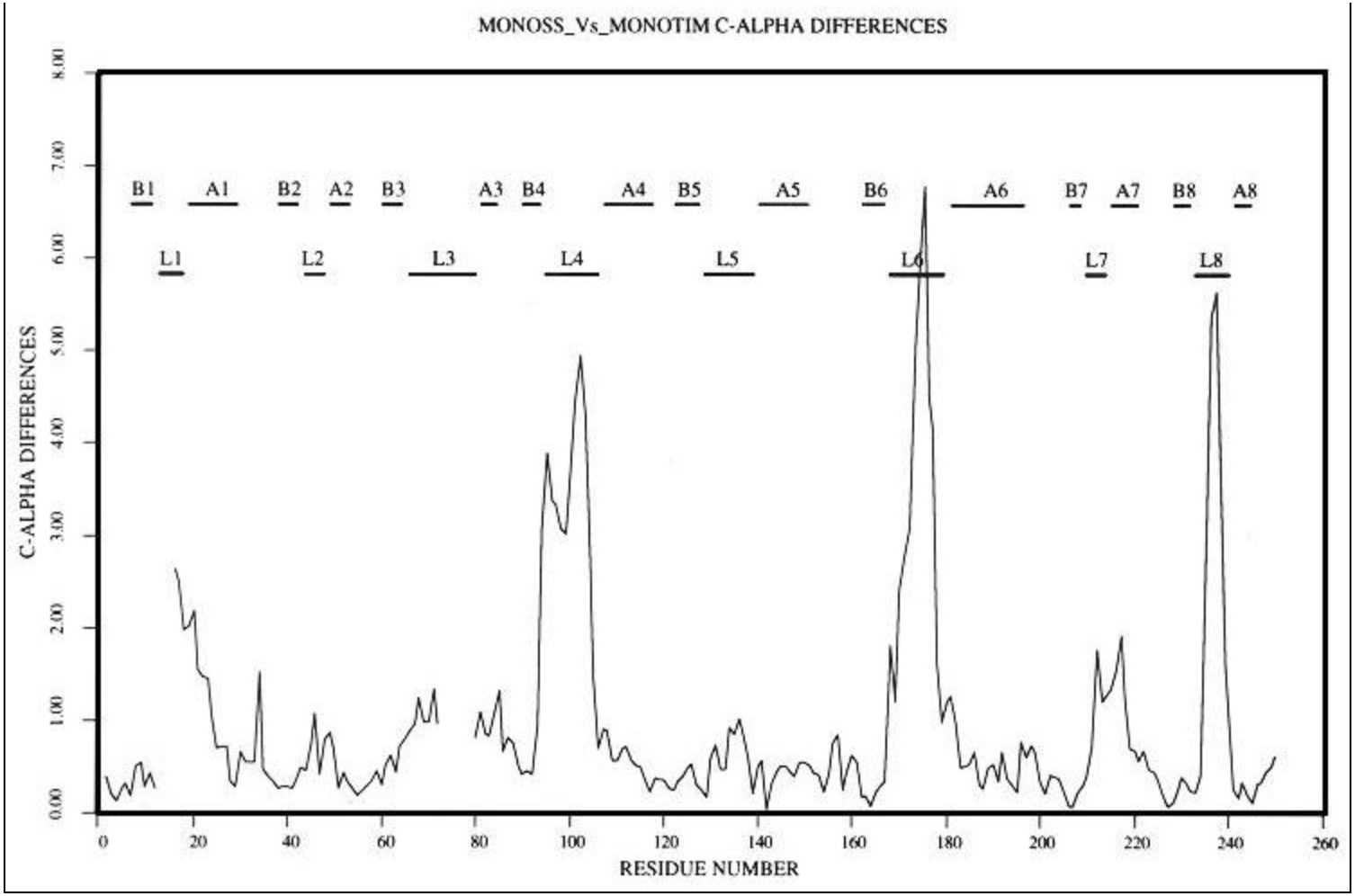

Fig. 3. The CΑ differences (in Å) between monoTIM-SS and monoTIM as a function of residue number. The break between residues 72 and 80 is due to the discontinuous numbering scheme for monoTIM (see legend to Fig. 2). The discontinuity near L1 is because some residues are missing in the models.

Return to text reference [1]

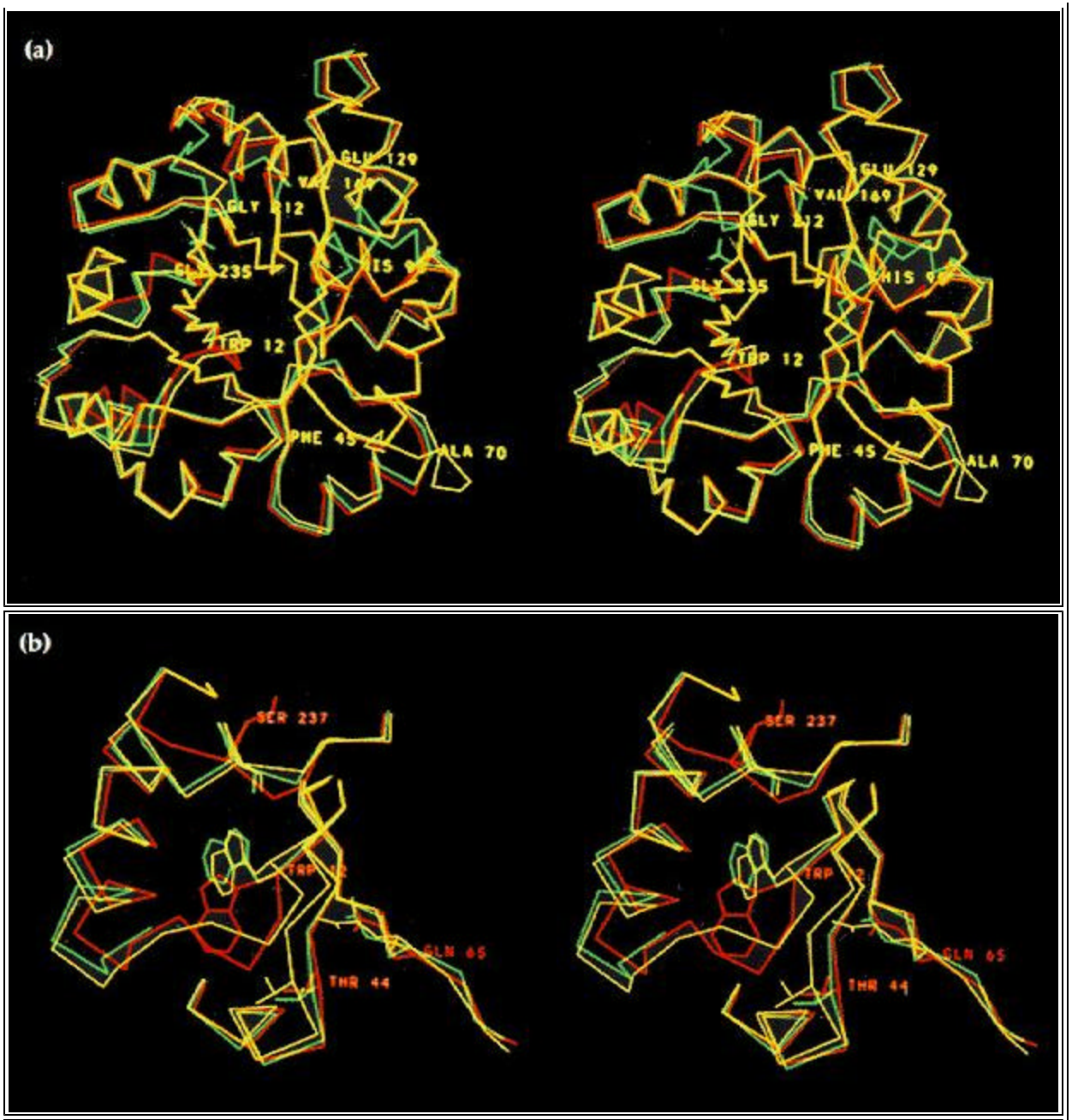

Fig. 4. Comparison of monoTIM-SS (red), monoTIM (green) and wtTIM (yellow). **(a)** The complete Cα traces. One residue of each front loop of monoTIM is labelled: Trp12 (L1), Phe45 (L2), Ala70 (L3), His95 (L4), Glu129 (L5), Val169 (L6), Gly212 (L7) and Gly235 (L8). Also shown, in green, is the sulphate ion, near loop-6, loop-7 and loop-8, as observed in the monoTIM structure. **(b)** Comparison of the Cα traces near L8, L1, L2 and L3. The side chains of residues

Ser237 (L8), Trp12 (L1), Thr44 (L2) and Gln65 (L3) are also shown.

Return to text reference [1] [2] [3] [4] [5] [6] [7] [8] [9]

The differences in loop L6, and also in the adjacent loops, L5 and L7, reflect the changes between the open conformation, observed in the monoTIM-SS structure and the closed conformation, observed in the monoTIM structure in complex with sulphate.

Major differences are also seen for loops L8 and L1. These loops are adjacent to each other (Fig. 4). L8 is important for the binding of the phosphate moiety of the substrate molecule. As can be seen in Fig. 4a, L8 has moved into the phosphate-binding pocket in monoTIM-SS. Because of this movement the interactions between loops L1 and L8 have been weakened. In particular, the hydrogen bonds between the carbonyl oxygen of Ser237 (L8) and Nε2 of Trp12 (L1) and between Oγ of Ser237 and the carbonyl oxygen of Asn11 (L1) have been lost, which apparently causes the observed rearrangement of the Trp12 side chain (Fig. 4b).

The χ_2 dihedral angle of Trp12 is close to zero in monoTIM (and wtTIM). This strained conformation of the Trp12 side chain is stabilized by the hydrogen bonds between loops L1 and L8 (described above), and also ensures a very good packing arrangement between these loops. This arrangement is lost in the monoTIM-SS structure, because rotation of the Trp12 side chain creates a large hydrophobic cavity (volume 60 Å^3). The cavity is lined solely by carbon side-chain atoms of Ala10, Trp12, Leu21, Ile25, Phe28, Val41 and Leu238. The rotation of the Trp12 side chain may not have an important effect on the stability, because the stabilizing effect (the removal of a strained dihedral angle) is counteracted by the creation of a hydrophobic cavity. The movement of the Trp12 side chain is facilitated by loop L2 being positioned further away from loop L1, as is also observed in monoTIM (Fig. 4b). In monoTIM-SS the polypeptide chain of loop L1 could be traced completely, but its trace differs greatly from those of monoTIM and wtTIM, such that the catalytic residue, Lys13, occupies an entirely different position. The conserved salt bridge between Lys13 and Glu97 in wtTIM is still present in this structure, but it has moved towards the solvent and 6 Å away from the active site. In the monoTIM-SS structure, the (φ,ψ) values of Lys13 (-135°, 172°) are unstrained, whereas in wtTIM these angles are (51°,–143°). The final difference between monoTIM and monoTIM-SS occurs in loop L4. In monoTIM-SS, L4 has adopted a similar conformation to that seen in wtTIM (Fig. 4a), that is, it is well ordered with average B-factor values (Fig. 5).

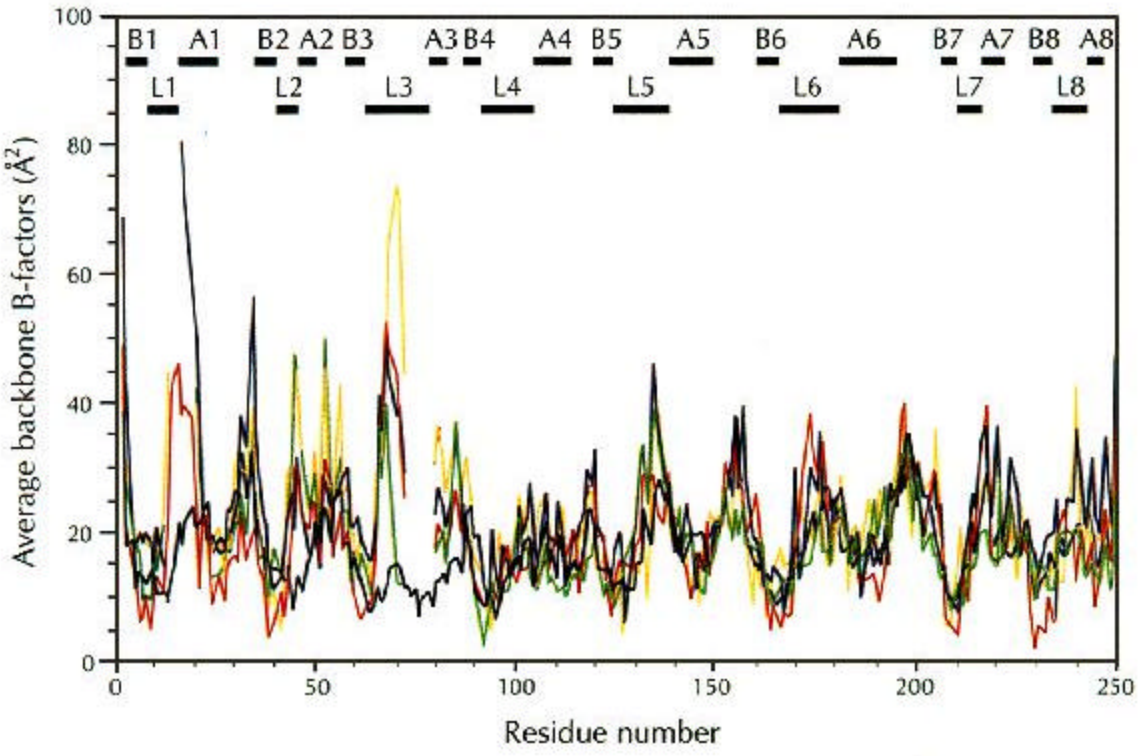

Fig. 5. B-factor plot of the main-chain atoms of subunit-1 of wtTIM (black), monoTIM (purple), monoTIM-SS (red), monoTIM-SS(PGH) (green) and monoTIM-W(2PG) (yellow). The discontinuity near L1 is because some residues are missing in the models; the break near L3 is due to the discontinuous numbering scheme of this loop in monoTIM (see legend to Fig. 2).

Return to text reference [1] [2] [3] [4] [5] [6]

Structure of monoTIM -SS in complex with PGH

In this structure a PGH molecule is bound in the active site (Fig. 6a) and loop L6 and those adjacent to it have adopted the closed conformation. The conformation of L8 is different from that found in monoTIM-SS, but the same as in monoTIM and wtTIM. The presence of the ligand in the active site appears to stabilize the wtTIM L8 conformation. Also, the Trp12 side chain again adopts the strained wild-type conformation. The major differences from the monoTIM structure occur in loops L4 and L1. As in the monoTIM-SS structure, L4 has again adopted the wtTIM conformation. In monoTIM-SS (PGH) residues 13–19 of L1 are disordered but, as is shown in Fig. 6a, the end of the side chain of Lys13 does have a preferred conformation, similar to that seen in wtTIM. As in monoTIM-SS the side chain of His95 has adopted a similar conformation to that of wtTIM. The side chain of Glu167 superimposes very well on that of the wtTIM glutamate. For example, the (χ^1, χ^2) angles of the Glu167 side chain are (-39°, -174°) and (-30°, -182°) for monoTIM-SS(PGH) and wtTIM(PGH), respectively, and the two carboxyl oxygen atoms superimpose to within 0.5 Å.

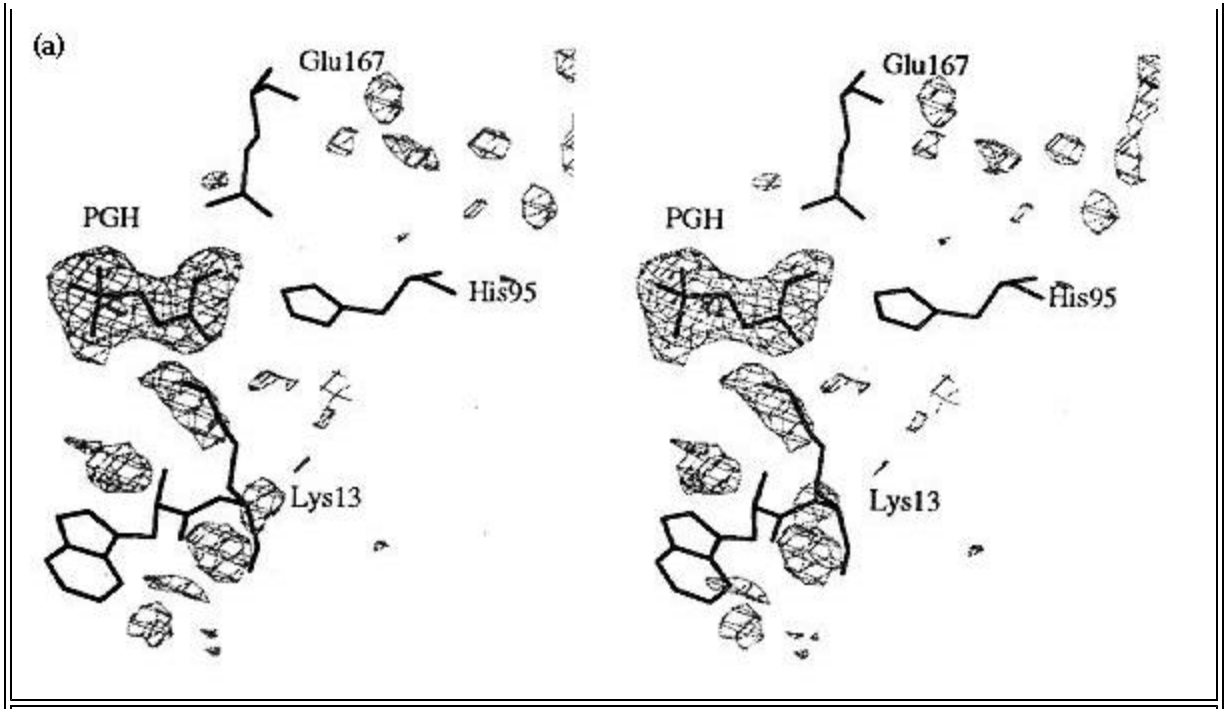
(a)
Glu167
PGH
His95
Lys13
Glu167
PGH
His95
Lys13

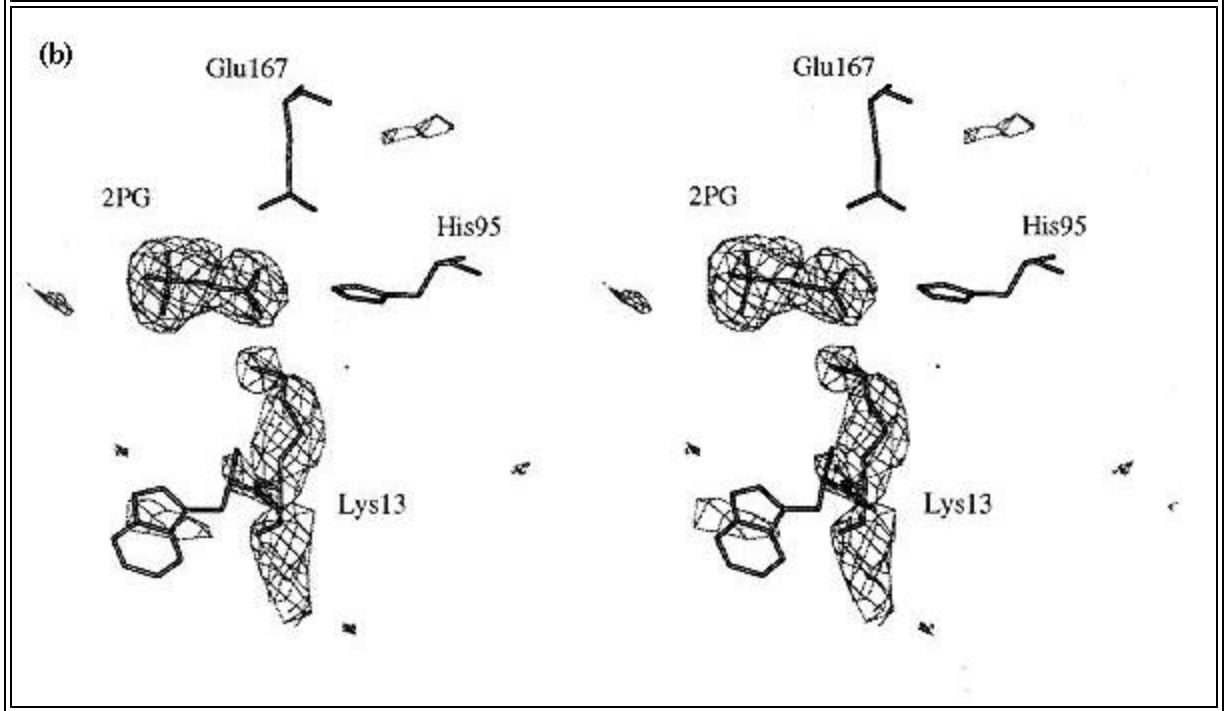
(b)
Glu167
2PG
His95
Lys13
Glu167
2PG
His95
Lys13

Fig. 6. Active site omit maps of monoTIM-SS(PGH) and monoTIM-W(2PG). The maps are F_o–F_c, α_c-maps contoured at three times the rms deviation from the mean. **(a)** PGH in omit density. F_c, α_c have been derived from the incomplete refined model, not yet containing residues 13–19 and the PGH molecule. The molecular fragments His95, Glu167 and PGH are from the completely refined monoTIM-SS(PGH) model; the fragment Trp12–Lys13 is from the wtTIM(PGH) complex. **(b)** 2PG in omit density. F_c, α_c have been calculated from the final model, but after removing 2PG and Lys13 from this model, followed by one cycle of positional and one cycle of B-factor refinement. The molecular fragments are from the final monoTIM-W(2PG) model.

Return to text reference [1] [2] [3] [4]

Structure of monoTIM -W in complex with 2PG

The side chain of tryptophan introduced at position 100 is clearly visible in the electron-density map (data not shown). It is in crystal contact with the equivalent side chain of a crystallographically related molecule. In this structure, 2PG is bound in the active site (Fig. 6b) and loop L6 and those adjacent to it have adopted the closed conformation. Loop L4 has a similar conformation to that seen in both monoTIM-SS structures. The conformations of L8 and Trp12 are similar to those in monoTIM and monoTIM-SS(PGH). Residues 14–19 of L1 are disordered. Interestingly, Lys13 is well ordered (Fig. 6b), but its main-chain conformation differs from that observed in wtTIM; its Φ angle is -110° in monoTIM-W(2PG) and 50° in wtTIM. Despite this difference in main-chain conformation, the side chain of Lys13 points in approximately the same direction as seen in wtTIM. However, there is no salt bridge between Lys13 and Glu97 (Fig. 7). The side chains of the catalytic histidine (His95) and glutamate (Glu167) are also in the same positions as in wtTIM (Fig. 7), as was observed for monoTIM-SS(PGH). The conformation of the 2PG molecule bound in the active site is well defined. PGH (in monoTIM-SS) and 2PG (in monoTIM-W) both bind in the active site in somewhat different conformations from those seen in complexes of wtTIM with these inhibitors (W Schliebs and RK Wierenga, unpublished data; Fig. 7).

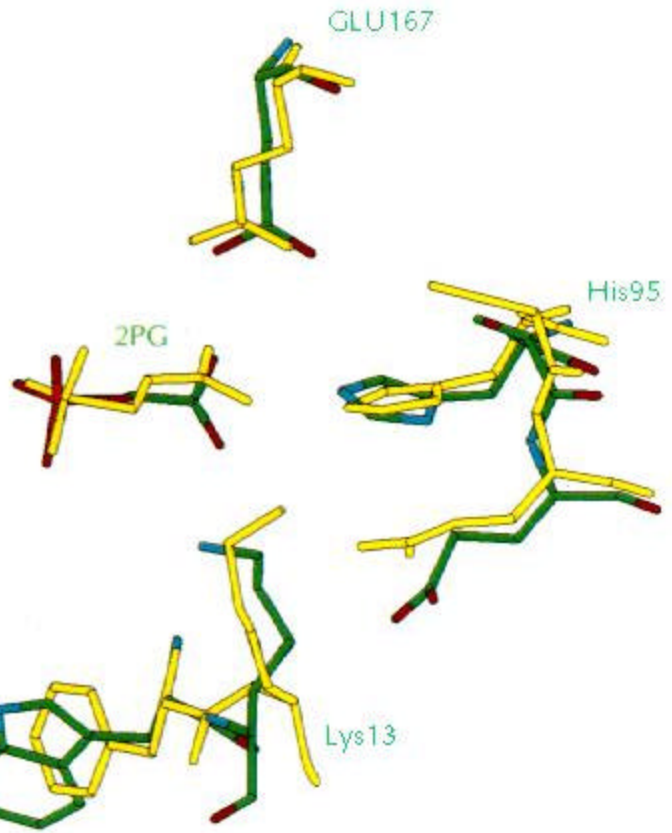

Fig. 7. Comparison of the mode of binding of 2PG in the active site of monoTIM-W(2PG) (in blue, green and red) and in yeast TIM (yellow) (2YPI in the PDB). In wtTIM Lys13 of L1 (on the left) forms a salt bridge with Glu97 of L4 (on the right). [Figure drawn with XOBJECTS (MEM Noble, Oxford University, unpublished program).].

Return to text reference [1] [2] [3] [4]

Discussion

The three new structures of the monoTIM variants have been crystallized under conditions which differ from each other and from those used for monoTIM (Table 1). Despite the structural differences, the dynamic properties of the different monomeric TIMs, as expressed in the variation of B-factor values, are remarkably similar (Fig. 5), with the β-strands 1–8 having low B-factors and the front and back loops having high B-factors. As can be seen in Fig. 5, this pattern of the B-factor values is also observed for wtTIM, with the important exception that in wtTIM the front loops L1–4 have low B-factors. In wtTIM these loops have the lowest B-factors of the entire structure, indicating that they are very rigid due to the interactions across the dimer interface.

The structural differences between the four structures of monomeric TIM must be adaptations to those experimental conditions that have been different, such as the introduction of point mutations,

the absence/presence of active-site ligand, variations in the mother liquor or differences in crystal contacts. From the structural analysis there is no evidence that the point mutations have caused the structural differences, in agreement with the observation that the kinetic constants are similar. For example, Fig. 4b shows that the Cα traces of loop L2 of monoTIM and monoTIM-SS are the same, despite the introduction of two serines in this loop. Similarly, there are no significant structural differences near residue 100 in loop L4, when comparing wtTIM, monoTIM-SS(PGH) and monoTIM-W (2PG) (Fig. 8a) despite the introduction of a tryptophan residue at this position.

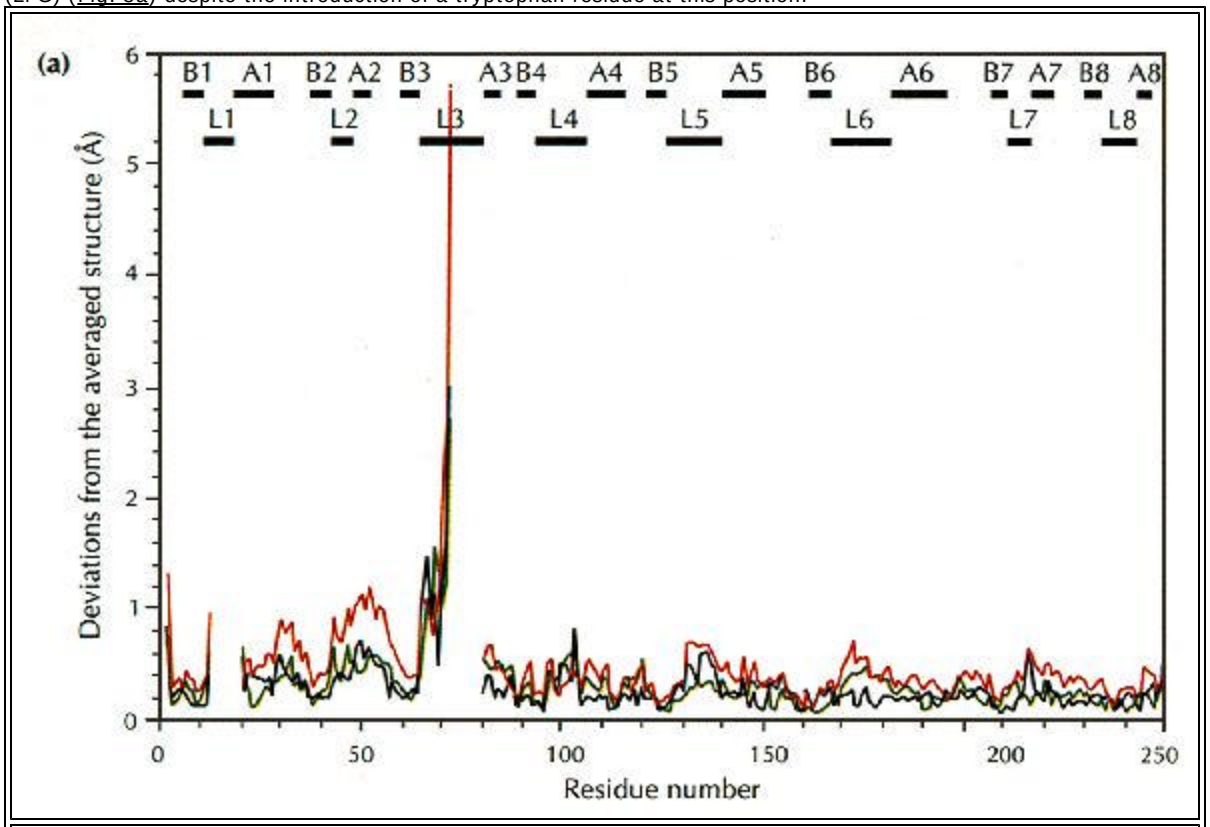

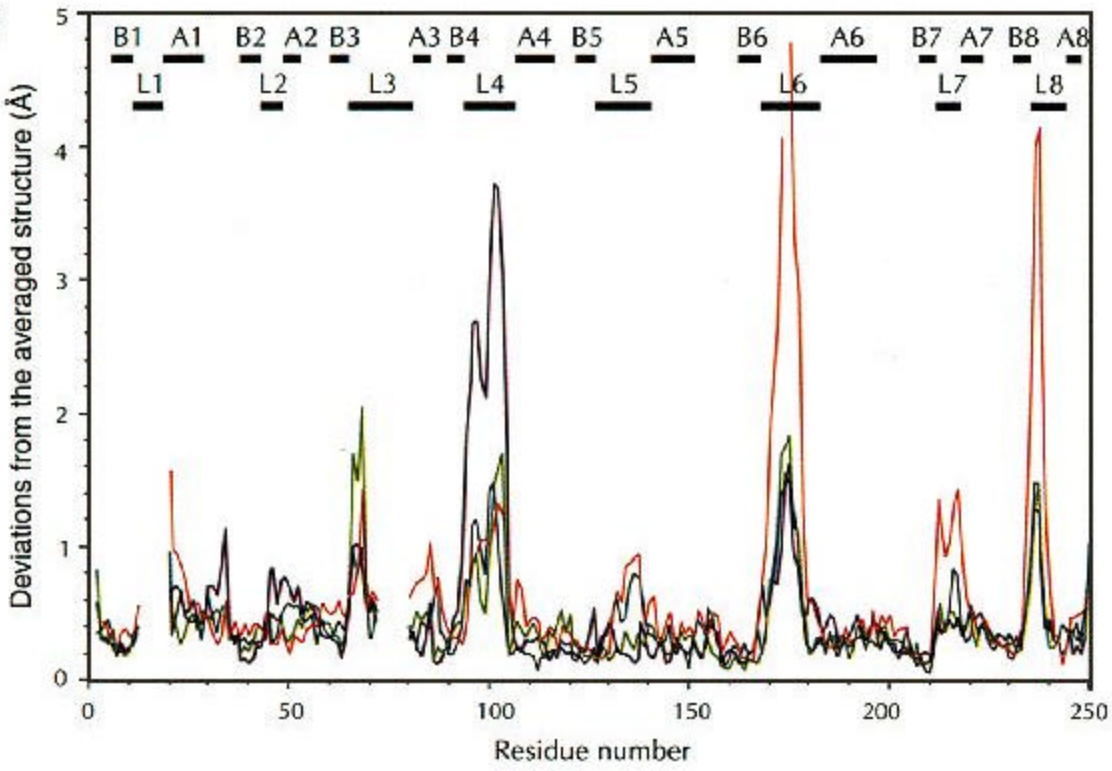

Fig. 8. Structural variability (calculated as described in the Materials and methods section). The discontinuity near L1 is because some residues are missing in the models; the break near L3 is due to the discontinuous numbering scheme of this loop in monoTIM (see legend to Fig. 2). **(a)** Deviations from the average structure for wtTIM(PGH) (red), monoTIM-SS(PGH) (green) and monoTIM-W(2PG) (black). The average structure is calculated from the coordinates of wtTIM(PGH), monoTIM-SS(PGH) and monoTIM-W(2PG). **(b)** Deviations from the average structure for monoTIM (blue), monoTIM-SS (red), monoTIM-SS(PGH) (green) and monoTIM-W(2PG) (black). The average structure is calculated from the coordinates of monoTIM, monoTIM-SS, monoTIM-SS(PGH) and monoTIM-W(2PG).

Return to text reference [1] [2] [3] [4]

The main-chain deviations of the four monomeric structures from their average structure (calculated as described in the Materials and methods section) are plotted in Fig. 8b. This illustrates that the structural differences occur almost exclusively in the front loops. The only exception is near residue 35 in back loop L1. However, this loop is ill defined; in the high-resolution wtTIM structure [3], as well as in the monomeric TIM structures, this loop has high B-factor values (Fig. 5). It can be seen in Fig. 8b that the average deviation from the mean structure is approximately 0.2 Å for the regions of the structure which have not changed at all (e.g. β-strands 5, 6, 7 and 8), whereas for the front loops L4, L6 and L8 deviations of 4 Å, 5 Å and 4 Å respectively, are observed.

The structural differences of loops L5, L6 and L7, as well as L8 correlate very well with the absence/presence of active-site ligands.

Crystal contacts

Crystal contacts seem to play an important role in determining the structure of loop L1. For example, in three structures [monoTIM, monoTIM-SS(PGH) and monoTIM-W(2PG)] a significant portion of L1, starting at Lys13 or Cys14 is completely mobile, but in monoTIM-SS the entire Cα trace for L1 could be built. In this structure, Cys14 and Asn15 are stabilized by crystal contacts (Table 3). This trace is, however, different from the wtTIM conformation (see Fig. 4a).

Table 3. Crystal contacts of the front loops in monomeric TIMs.

Loop	monoTIM	monoTIM -SS	monoTIM -SS(PGH)	monoTIM -W(2PG)
L1 (12–17)	0	20	0	0
L2 (44–47)	15	6	0	0
L3 (65–72)	4	10	26	0
L4 (94–105)	60	30	28	77
L5 (128–138)	1	12	5	5
L6 (167–179)	0	9	13	22
L7 (211–215)	0	0	0	0
L8 (234–241)	0	7	0	0

The crystal contacts are the number of atom–atom contacts within 4 Å between the central molecule and its neighbouring molecules in the crystal.

Return to table reference [1] [2] [3] [4]

Loop L4 is observed in two conformational states (in monoTIM it is an 'out' position, in monoTIM-SS, monoTIM-SS(PGH) and monoTIM-W(2PG) it is an 'in' position, as in the wild-type protein [8]). As shown in Table 3, L4 is involved in crystal contacts in all four structures. In each structure L4 is well defined, with average B-factor values (Fig. 5). As crystal contact forces are weak, it seems likely that the conformational flexibility of L4 arises from the existence of two preferred states in solution, of approximately equal stability, separated by a low energy barrier, rather than from its being an ill defined and mobile loop region, as is the case for loop L1.

It is of note that loops L1–4 are more important for the stability of the crystal (276 crystal contacts; Table 3), despite their assumed mobility in solution, than loops L5–8 (74 crystal contacts; Table 3).

Comparison with wtTIM

The conformational flexibility of loops L1, L4 and L8 in monoTIM is not observed in wtTIM. Several crystal structures of wtTIM have been described, including chicken [10], yeast [11], trypanosomal [3], *Escherichia coli* [12] and human [13] TIMs. From these wild-type structures it has been found that the position of loop L6 and also of the adjacent loops, L5 and L7, depends on the absence or presence of an active-site ligand [14]. However, in all these wild-type structures loops L1, L4 and L8 are well defined and always adopt the same conformation. Clearly, the monomerization, arising from the deletion in L3, has caused this enhanced flexibility of loops L1, L4 and L8. In wtTIM, the conformation of L8 is stabilized by interactions with L1, as described above. The conformations of L1 and L4 in wtTIM are stabilized at the dimer interface only by interactions with L3 of the other subunit, because the tip of L3 binds within a pocket shaped by L1 and L4 of the first subunit. Across the dimer interface there are 50 L1–L3 atom pairs and 45 L4–L3 atom pairs within a 4 Å cutoff. These tight interactions stabilize the strained conformation of Lys13 (Φ=51°, Ψ=-143°), as observed in all

known wild-type structures. The dimer-interface interactions cause L1 and L4 to be very rigid, as is clear from the B-factor plot of wtTIM (Fig. 5). In the structures of monomeric TIMs, Lys13 is either mobile, or has adopted structures with a negative (unstrained) value for Φ [in monoTIM-SS and monoTIM-W(2PG)], indicating that the dimer-interface interactions are required to stabilize the strained conformation of Lys13 in the wild-type structure. The increased flexibility of loops L1, L4 and L8 in monoTIM could be due to the shortening of L3 alone, but is probably caused by the monomerization itself. The first possibility does not seem very likely, because the changed residues of wild-type loop L3 (residues 68–82; [6] [8]) do not interact with any atom of L1 or L4 of the same subunit.

In wtTIM, L6, together with the adjacent loops L5 and L7, can be in an open or closed state. In the monomeric TIM structures, the open structure is observed for monoTIM-SS and the closed structure is observed for monoTIM-SS(PGH), monoTIM-SS(2PG) and monoTIM in complex with sulphate. Clearly, the open/closed mechanism still operates in monomeric TIM and in the closed form the catalytic glutamate, Glu167, at the beginning of L6, adopts the same conformation as in wtTIM. What is different in monomeric TIM is the flexibility of loops L1, L4 and L8. Loop L8 is only different from wtTIM in the monoTIM-SS structure and loop L4 is only different in the monoTIM structure (Fig. 4a). The structure of monoTIM-W(2PG) shows that both Lys13 (L1) and His95 (L4) can adopt conformations similar to those seen in wtTIM (Fig. 7). In wild type, Lys13 is important for binding the substrate [15]. The exact role of Lys13 in the catalysis has not yet been established [16] [17], but mutational analysis has shown that any positively charged side chain at this position permits some catalytic activity, demonstrating the importance of the overall electrostatic properties of the active-site pocket [15]. His95 is important for the proton shuffling between the two oxygen atoms of the substrate [17] [18] [19]. The structures of monoTIM-SS(PGH) and monoTIM-W(2PG) indicate that the side chains of Lys13 and His95 can play the same role in catalysis as in wild type.

Apart from the increased flexibility of the front loops, at least one other difference exists between the active sites of monoTIM and wtTIM that will also influence the catalytic efficiency. In wtTIM, the active-site pocket is shielded from bulk solvent by the other subunit, but in monoTIM the active site is much more exposed to bulk solvent, and this will affect its dielectric properties.

The three different monoTIMs have very similar catalytic properties despite the structural differences seen in the various crystal forms. This is consistent with the conclusion that the active-site loops are mobile in solution, and that the loop conformations seen in the crystal structures are induced by the crystallization conditions. We might imagine two kinds of mobility in solution: firstly, fast switches between two (or more) discrete conformational states (as might be the case for L4) and secondly, 'continuous flexibility' (as discussed for L1). Without performing experiments in solution (e.g. using NMR), it is hard to discriminate between these two possibilities at the present time.

Biological implications

Triosephosphate isomerase (TIM) is a dimeric enzyme. Each subunit consists of eight ($\beta\alpha$) units connected by loops. The loops following the β-strands (loops L1–8) are the so-called 'front' loops. The dimer is stabilized by tight interactions between the residues of the four dimer-interface loops, L1–4. Two important catalytic residues, Lys13 (on L1) and His95 (on L4), reside on these dimer-interface loops. In this study we have analyzed the structural properties of these loops in TIMs engineered to form stable monomers (monoTIMs).

In the wild-type (wt) TIM dimer these loops are very rigid, but in our comparison of four crystal structures of monoTIMs these loops are seen to exhibit remarkable conformational flexibility. Nevertheless, the monoTIMs have residual catalytic activity. This apparent paradox is explained by our observation that the catalytic residues on these loops can adopt conformations similar, although not identical, to those in wtTIM, in the presence of active-site ligands.

The flexibility of loops L1, L4 and L8 in monoTIM implies that in wild-type subunits, free in solution, these loops are also flexible. The sequence of the monoTIMs differ from wtTIM by the deletion of seven residues from the interface loop, L3. It is very likely that the observed conformational flexibility of loops L1, L4 and L8 in monoTIM is caused by the absence of the other subunit rather than the deletion itself. If this is the case, then the assembly of unfolded wtTIM monomers into dimers follows a path, in agreement with a consecutive folding-association mechanism [20]: firstly, the monomers adopt a folded structure, in which the interface loops are still mobile (as inferred from these studies); secondly, these monomers recognize each other and subsequently undergo further structural reshuffling, leading to the final tertiary and quaternary structure. Further characterization of point-mutation variants of wtTIM, engineered to make dimerization impossible, will be required to confirm this hypothesis.

The flexibility of some of the front loops in monoTIM has the following implication for designing monoTIMs with increased catalytic activity. Sequence changes in loops L1 and L4 (or their immediate environments) which increase their rigidity and hence allow the active-site residues to adopt wild-type conformations, should enhance the catalytic activity of monoTIM. Protein design experiments targeting loop L1 have been initiated.

Materials and methods

DNA technology, protein expression and protein purification

E. coli strains XL1-Blue [21] and BL21(DE3) [22] were used as hosts for the plasmids throughout the genetic manipulations and the expression of the proteins, respectively. The plasmids encoding the variant proteins were, except for the mutations in the TIM gene, identical to plasmid pTIM described previously [23]. For monoTIM-SS, serine codons were introduced by site-directed mutagenesis at positions 45 and 46 in the monoTIM gene, located on plasmid pTIM [23]. MonoTIM-W is derived from monoTIM by changing the alanine at position 100 into a tryptophan. The site-directed mutagenesis was done by the polymerase chain reaction (PCR) using the overlap-extension procedure [24]. The DNA sequences of the cloned PCR-amplified fragments were verified. MonoTIM-SS and monoTIM-W expression and purification to homogeneity were carried out as described for monoTIM [6]. The kinetic constants were measured in a coupled enzyme assay as previously described [7].

Crystallization and data collection

The monoTIM-SS and monoTIM-W crystals were grown at room temperature using the hanging drop method. The crystallization conditions for monoTIM-SS, monoTIM-SS(PGH), and monoTIM-W(2PG) crystals (Table 1) were found by a standard screening procedure [25]. One crystal was used for each dataset. The data were collected at room temperature with a FAST area detector, mounted on a rotating anode. Data processing was performed with MADNES [26]. The data collection statistics are summarized in Table 2.

Structure determination and refinement

MonoTIM-SS: The structure was solved by molecular replacement using the CCP4 program package [27]. The self-rotation function (10–4 Å) gave a very clear peak for a local twofold axis. As a search model for the molecular replacement calculations subunit -1 of the 1.83 Å refined structure of trypanosomal TIM [5TIM in the Brookhaven Protein Data Bank (PDB)] was used, after omitting the residues of loops L1, L3, L4, and L6. The molecular replacement calculations gave a clear indication of the orientation and position of the two monoTIM-SS molecules. The starting model was rebuilt in a 3 Å map using O [28], and refined with X-PLOR [29] first at 3 Å and subsequently at higher

resolution. The missing loops were gradually added back to the model. All the maps used for model building were SIGMAA-weighted [30] $2mF_o–DF_c$ maps. Once the complete model was built, the refinement was continued at 2.4 Å resolution with the TNT package [31], which was also used for the restrained refinement of individual B-factors. Water molecules were added after analyzing peaks in the $F_o–F_c$ map. Peaks were only interpreted as water molecules when peaks in the $F_o–F_c$ map were also present in the $2mF_o–DF_c$ map, and only when such waters were in hydrogen-bonding contact with polar protein atoms. The relative positions of the two monoTIM-SS molecules is such that the side chains of Cys14 of the two molecules in the asymmetric unit come close together, but the geometry of the main chain in this region seems incompatible with an undistorted cystine SS-bridge. Therefore, these two cysteines were refined as alanines. The final $2mF_o–DF_c$ map of this region lacks peaks of high density, suggesting crystallographic disorder for the two cysteines. The R-factor of the final model is 19.8% (Table 2).

MonoTIM-SS(PGH): Crystals were grown in the presence of PGH, synthesized according to Collins [32]. The synthesized PGH was purified by ion-exchange chromatography on Q-Sepharose. NMR and mass spectrometric measurements show that the final sample is predominantly PGH, but small amounts of the starting material could be detected. The crystals diffracted rather well and a 2.4 Å dataset (86% complete) could be collected. The structure was solved by the method of molecular replacement, using CCP4 software, as described above for monoTIM-SS. The monoTIM structure (1TRI in the PDB) was used as a search model, after omitting the residues of loops L1, L3, L4 and L6. The truncated monoTIM model was positioned in the monoTIM-SS(PGH) cell and the first model building and refinement (using X-PLOR) was performed with 3 Å data. As the refinement proceeded, loops L3, L4 and L6 were gradually modelled into their corresponding densities. However, for L1, no clear density was present for residues 13–19, even on complete refinement of the rest of the protein. At this stage of the refinement, when the PGH molecule had not yet been included in the model, clear density was observed for an inhibitor molecule in the active site. A refinement cycle was first carried out with a 2PG molecule built into this density, but in the subsequent $F_o–F_c$ map there was clearly residual density for the extra PGH atom (Fig. 1b). Therefore a model of PGH was constructed, using INSIGHT (Biosym Inc., San Diego, CA), and built in the corresponding density. This PGH model was included in the refinement calculations, which resulted, after further refinement, in the final model (Table 2).

MonoTIM-W(2PG): The structure was solved using molecular replacement calculations, as described above. The monoTIM structure was used as a search model, after omitting residues of loops L1, L3, L4 and L6. The first model building was performed in a 3 Å map and the initial refinement was done with X-PLOR, first at 3 Å resolution and subsequently at increasingly higher resolution. TNT was used for the high-resolution refinement at 2.4 Å. As the refinement proceeded, loops L3, L4 and L6 were gradually added back to the model. No clear density was present for residues 14–19 of loop L1. When the complete protein model was refined, 12 water molecules were added. At this stage there was clear density for the 2PG molecule. A 2PG molecule, with geometry as determined crystallographically [33], was built in this density and included in the refinement (Table 2).

Structure analysis

The structures have been analyzed with O [28] and WHAT IF [34]. The residue numbering scheme of the monomeric TIMs is the same as in wtTIM, therefore (due to the L3 deletion) residue 72 is covalently connected to residue 80 [8]. For the comparisons the 2.5 Å structure of monoTIM (1TRI in the PDB), the 1.83 Å structure of wtTIM (5TIM in the PDB), and the 2.5 Å structure of the wtTIM (PGH) complex (1TRD in the PDB) have been used. The 105 Cα atoms of the framework strands and helices (as defined previously [35]) have been used for the superpositions. Hydrogen-bond calculations and cavity calculations were performed with WHAT IF [34] and the MSP package [36], respectively, using the same parameters as in previous calculations [35]. The deviations from the average structures, as presented in Fig. 8, have been calculated for each residue from the four main-chain atoms. First, the average positions were calculated for every atom from a selected set of

structures. Subsequently, the distance was calculated from individual atom positions to the average atom position. For each residue of each structure the distances of the four main-chain atoms are averaged and plotted.

The coordinates of monoTIM-SS (1MSS), monoTIM-SS(PGH) (1TTJ) and monoTIM-W(2PG) (1TTI) have been deposited in the Brookhaven Protein Data Bank.

Acknowledgments

We thank Drs Sproat and Douglas (EMBL) for their help with the synthesis of PGH and the referee for valuable comments. This work was supported by an EC-BRIDGE-grant (BIOT-CT90-0182).

References

1. Knowles J.R. : 1991,
Enzyme catalysis: not different, just better.
Nature **350** : 121–124. MEDLINE Cited by
Return to citation reference [1]

2. Lolis E. , Petsko G.A. : 1990,
Crystallographic analysis of the complex between triosephosphate isomerase and 2 -phosphoglycolate at 2.5 -Å resolution: implications for catalysis.
Biochemistry **29** : 6619–6625. MEDLINE Cited by
Return to citation reference [1]

3. Wierenga R.K. , Noble M.E.M. , Vriend G. , Nauche S. , Hol W.G.J. : 1991,
Refined 1.83 Å structure of trypanosomal triosephosphate isomerase crystallized in the presence of 2.4 M -ammonium sulphate. A comparison with the structure of the trypanosomal triosephosphate isomerase -glycerol -3-phosphate complex.
J. Mol. Biol. **220** : 995–1015. MEDLINE Cited by
Return to citation reference [1] [2] [3] [4] [5]

4. Joseph D. , Petsko G.A. , Karplus M. : 1990,
Anatomy of a conformational change: hinged 'lid' motion of the triosephosphate isomerase loop.
Science **249** : 1425–1428. MEDLINE Cited by
Return to citation reference [1]

5. Urfer R. , Kirschner K. : 1992,
The importance of surface loops for stabilizing an eightfold βα barrel protein.
Protein Sci. **1**: 31–45. MEDLINE Cited by
Return to citation reference [1]

6. Borchert T.V. , Abagyan R. , Jaenicke R. , Wierenga R.K. : 1994,
Design, creation, and characterization of a stable, monomeric triosephosphate isomerase.
Proc. Natl. Acad. Sci. USA **91** : 1515–1518. MEDLINE Cited by
Return to citation reference [1] [2] [3]

7. Lambeir A.-M. , Opperdoes F.R. , Wierenga R.K. : 1987,
Kinetic properties of triose -phosphate isomerase from *Trypanosoma brucei brucei.* A comparison with the rabbit muscle and yeast enzymes.
Eur. J. Biochem. **168** : 69–74. MEDLINE Cited by
Return to citation reference [1] [2]

8. Borchert T.V. , Abagyan R. , Radha Kishan K.V. , Zeelen J.Ph. , Wierenga R.K. : 1993,
The crystal structure of an engineered monomeric triosephosphate isomerase, monoTIM: the correct modelling of an eight -residue loop.
Structure **1**: 205–213. Cited by
Return to citation reference [1] [2] [3] [4] [5]

9. Radha Kishan K.V. , Zeelen J.P. , Noble M.E.M. , Borchert T.V. , Wierenga R.K. : 1994,
Comparison of the structures and the crystal contacts of trypanosomal triosephosphate isomerase in four different crystal forms.
Protein Sci. **3**: 77–787. Cited by
Return to citation reference [1]

10. Banner D.W. et al , Waley S.G. : 1975,
Structure of chicken muscle triose phosphate isomerase determined crystallographically at 2.5 Å resolution using amino acid sequence data.
Nature **255** : 609–614. MEDLINE Cited by
Return to citation reference [1]

11. Lolis E. , Alber T. , Davenport R.C. , Rose D. , Hartman F.C. , Petsko G.A. : 1990,
Structure of yeast triosephosphate isomerase at 1.9 Å resolution.
Biochemistry **29** : 6609–6618. MEDLINE Cited by
Return to citation reference [1]

12. Noble M.E.M. , Zeelen J.P. , Wierenga R.K. : 1993,
Structure of triosephosphate from *Escherichia coli* determined at 2.6 Å resolution.
Acta Crystallogr. D **49**: 403–417. Cited by
Return to citation reference [1]

13. Mande S.C. , Mainfroid V. , Kalk K.H. , Goraj K. , Martial J.A. , Hol W.G.J. : 1994,
Crystal structure of recombinant human triosephosphate isomerase at 2.8 Å resolution.
Protein Sci. **3**: 810–821. MEDLINE Cited by
Return to citation reference [1]

14. Wierenga R.K. , Borchert T.V. , Noble M.E.M. : 1992,
Crystallographic binding studies with triosephosphate isomerases: conformational changes induced by substrate and substrate -analogues.
FEBS Lett. **307** : 34–49. MEDLINE Cited by
Return to citation reference [1]

15. Lodi P.J. , Chang L.C. , Knowles J.R. , Komives E.A. : 1994,
Triosephosphate isomerase requires a positively charged active site: the role of lysine -12.
Biochemistry **33** : 2809–2814. MEDLINE Cited by
Return to citation reference [1] [2]

16. Joseph-McCarthy D. , Lolis E. , Komives E.A. , Petsko G.A. : 1994,
Crystal structure of the K12M/G15A triosephosphate isomerase double mutant and electrostatic analysis of the active site.
Biochemistry **33** : 2815–2823. MEDLINE Cited by
Return to citation reference [1]

17. Bash P.A. , Field M.J. , Davenport R.C. , Petsko G.A. , Ringe D. , Karplus M. : 1991,
Computer simulation and analysis of the reaction pathway of triosephosphate isomerase.
Biochemistry **30** : 5826–5832. MEDLINE Cited by
Return to citation reference [1] [2]

18. Komives E.A. , Chang L.C. , Lolis E. , Tilton R.F. , Petsko G.A. , Knowles J.R. : 1991,
Electrophilic catalysis in triosephosphate isomerase: the role of histidine -95.
Biochemistry **30** : 3011–3019. MEDLINE Cited by
Return to citation reference [1]

19. Lodi P.J. , Knowles J.R. : 1991,
Neutral imidazole is the electrophile in the reaction catalyzed by triosephosphate isomerase: structural origins and catalytic implications.
Biochemistry **30** : 6948–6956. MEDLINE Cited by
Return to citation reference [1]

20. Zabori S. , Rudolph R. , Jaenicke R. : 1980,
Folding and association of triose phosphate isomerase from rabbit muscle.
Z. Natur-forsch. [C] **35** : 999–1004.
Return to citation reference [1]

21. Bullock W.O. , Fernandez J.M. , Short J.M. : 1987,
XL1-Blue: a high efficiency plasmid transforming *recA Escherichia coli* strain with beta-galactosidase selection.
Biotechniques **5** : 376–378. Cited by
Return to citation reference [1]

22. Studier F.W. , Moffatt B.A. : 1986,
Use of the bacteriophage T7 RNA polymerase to direct selective high -level expression of cloned genes.
J. Mol. Biol. **189** : 113–130. MEDLINE Cited by
Return to citation reference [1]

23. Borchert T.V. et al , Wierenga R.K. : 1993,
Overexpression of trypanosomal triosephosphate isomerase in *Escherichia coli* and characterisation of a dimer -interface mutant.
Eur. J. Biochem. **211** : 703–710. MEDLINE Cited by
Return to citation reference [1] [2]

24. Higuchi R. , Krummel B. , Saiki R.K. : 1988,
A general method of *in vitro* preparation and specific mutagenesis of DNA fragments: study of protein and DNA interactions.
Nucleic Acids Res. **16** : 7351–7367. MEDLINE Cited by
Return to citation reference [1]

25. Zeelen J.P. , Hiltunen J.K. , Ceska T.A. , Wierenga R.K. : 1994,
Crystallization experiments with 2 -enoyl-CoA hydratase, using an automated 'fast -screening' crystallization protocol.
Acta Crystallogr. D **50** : 443–447. Cited by
Return to citation reference [1]

26. Messerschmidt A. , Pflugrath J.W. : 1987,
Crystal orientation and X -ray pattern prediction for area detector diffractometer systems in macromolecular crystallography.
J. Appl. Crystallogr. **20** : 306–315. Cited by
Return to citation reference [1]

27. Collaborative Computational Project Number 4: 1994,
The CCP4 suite: programs for protein crystallography.
Acta Crystallogr. D **50** : 760–763. Cited by
Return to citation reference [1]

28. Jones T.A. , Zou J.-Y. , Cowan S.W. , Kjeldgaard M. : 1991,
Improved methods for building protein models in electron density maps and the location of errors in these models.
Acta Crystallogr. A **47** : 110–119. Cited by
Return to citation reference [1] [2]

29. Brünger A.T. : 1992, *X-PLOR: Version 3.1, A System for X-ray Crystallography and NMR.* Yale University Press, New Haven and London:
Return to citation reference [1]

30. Read R.J. : 1986,
Improved Fourier coefficients for maps using phases from partial structures with errors.
Acta Crystallogr. A **42** : 140–149. Cited by
Return to citation reference [1]

31. Tronrud D.E. : 1992,
Conjugate -direction minimization: an improved method for the refinement of macromolecules.
Acta Crystallogr. A **48** : 912–916. Cited by
Return to citation reference [1]

32. Collins K.D. : 1974,
An activated intermediate analogue. The use of phosphoglycolohydroxamate as a stable analogue of a transiently occurring dihydroxyacetone phosphate -derived enolate in enzymatic catalysis.
J. Biol. Chem. **249** : 136–142. MEDLINE Cited by
Return to citation reference [1]

33. Lis T : 1993,
Structure of phosphoglycolate (PG) in different ionization states.
Acta Crystallogr. C **49** : 696–705. Cited by
Return to citation reference [1]

34. Vriend G. : 1990,
WHAT IF: a molecular modeling and drug design program.
J. Mol. Graphics **8** : 52–56. MEDLINE Cited by
Return to citation reference [1] [2]

35. Wierenga R.K. , Noble M.E.M. , Davenport R.C. : 1992,
Comparison of the refined crystal structures of liganded and unliganded chicken, yeast and trypanosomal triosephosphate isomerase.
J. Mol. Biol. **224** : 1115–1126. MEDLINE Cited by
Return to citation reference [1] [2]

36. Connolly M.L. : 1985,
Computation of molecular volume.
J. Am. Chem. Soc. **107** : 1118–1124. Cited by
Return to citation reference [1]

Received / Accepted

Received: 29 Mar 1995
Revisions requested: 26 Apr 1995
Revised: 4 May 1995
Accepted: 4 May 1995
Electronic revisions: PDB links created: 2YPI (extlink), 5TIM (extlink), 1TRD (extlink), 1MSS

(extlink), 1TTJ (extlink), 1TTI (extlink)

Author Contacts

Torben V Borchert, KV Radha Kishan, Johan Ph Zeelen, Wolfgang Schliebs, Narmada Thanki, Ruben Abagyan and Rik K Wierenga (corresponding author), EMBL, Postfach 102209, D-60912 Heidelberg, Germany. Rainer Jaenicke, Institut für Biophysik und Physikalische Biochemie, Universtät Regensburg, D-93040 Regensburg, Germany. Present address for Torben V Borchert: Novo-Nordisk A/S, Industrial Biotechnology, Novo Allé, DK-2880 Bagsvaerd, Denmark. Present address for Ruben Abagyan: The Skirball Institute for Biomolecular Medicine, New York, NY 10016, USA.

Return to author list

Copyright